



# Chronic Leptin Treatment Induces Epithelial-Mesenchymal Transition in MCF10A Mammary Epithelial Cells

Juan Carlos Juárez-Cruz<sup>1</sup> · Michal Okoniewski<sup>2</sup> · Mónica Ramírez<sup>3</sup> · Carlos Ortuño-Pineda<sup>4</sup> · Napoleón Navarro-Tito<sup>1</sup> · Eduardo Castañeda-Saucedo<sup>1</sup>

Received: 4 July 2021 / Accepted: 8 February 2022 / Published online: 23 February 2022  
© The Author(s), under exclusive licence to Springer Science+Business Media, LLC, part of Springer Nature 2022

## Abstract

Leptin is a cytokine-like hormone that functions as a link between obesity and breast cancer (BC). Leptin treatment induces Epithelial to Mesenchymal Transition (EMT) in BC cell lines. In non-tumoral breast epithelial MCF10A cells, acute leptin treatment induces partial EMT. However, the effect of chronic leptin treatment on EMT in non-tumorigenic breast cells has not been fully explored. This study aimed to evaluate the effect of chronic leptin treatment on the induction of EMT in MCF10A cells. We found that chronic leptin treatment induces a switch from an epithelial to a mesenchymal morphology, partial loss of E-cadherin and gain of vimentin expression. Immunolocalization experiments showed a partial loss of E-cadherin at cell junctions and increased cytoplasmic localization of vimentin in leptin-treated cells. Moreover, chronic leptin treatment increased collective cell migration and invasion. Furthermore, when cultured in non-adherent conditions leptin treated cells exhibited reduced cell aggregation, increased survival, and decreased apoptosis, which correlates with increased FAK and AKT phosphorylation. Finally, bioinformatic analysis in two publicly available RNAseq datasets from normal breast tissue shows that high levels of leptin mRNA correlate positively with the expression of mesenchymal markers, and negatively with epithelial markers. Thus, our results demonstrate that chronic leptin treatment induces EMT in non-tumorigenic MCF10A cells and suggest that high leptin expression in normal breast tissue may induce EMT and contribute to increased risk of breast cancer.

**Keywords** Breast cancer · Chronic-leptin · EMT · MCF10A

## Introduction

Breast cancer (BC) is the most common type of invasive cancer and the leading cause of death from malignant neoplasia in women worldwide (<https://gco.iarc.fr/>). Furthermore, epidemiological studies show that obesity is a relevant

risk factor for the development and progression of BC [1–3]. The adipose tissue functions as an endocrine organ, secreting proinflammatory cytokines, steroid hormones, and adipokines that activate essential signaling pathways involved in BC progression [4, 5].

✉ Eduardo Castañeda-Saucedo  
ecastaneda@uagro.mx  
Juan Carlos Juárez-Cruz  
jcjuarez91@gmail.com  
Michal Okoniewski  
michal.okoniewski@id.ethz.ch  
Mónica Ramírez  
mramirezru@conacyt.mx  
Carlos Ortuño-Pineda  
carlos2pineda@hotmail.com  
Napoleón Navarro-Tito  
nnavarro@uagro.mx

<sup>1</sup> Laboratorio de Biología Celular del Cáncer. Facultad de Ciencias Químico-Biológicas, Universidad Autónoma de Guerrero. Av. Lázaro Cárdenas S/N Ciudad Universitaria. C.P. 39087, Chilpancingo de los Bravo, Guerrero, México  
<sup>2</sup> Scientific IT Services ETH Zurich, ETH Zurich, Zürich, Switzerland  
<sup>3</sup> CONACYT, Universidad Autónoma de Guerrero, Chilpancingo de los Bravo, Guerrero, México  
<sup>4</sup> Laboratorio de Ácidos Nucleicos y Proteínas. Facultad de Ciencias Químico-Biológicas, Universidad Autónoma de Guerrero, Chilpancingo de los Bravo, Guerrero, México

Leptin is a non-glycosylated 16 kDa protein encoded by the LEP gene. It is a cytokine-like hormone that is recognized as a link between obesity and BC [6, 7]. Adipose tissue is the primary source for leptin production, and increased expression/secretion of leptin by adipose tissue is positively associated with overweight and obesity [8, 9]. Interestingly, it has been shown that serum leptin levels are higher in patients with BC than in individuals without BC [10–12]. Moreover, both leptin and leptin receptor protein levels are higher in breast tumors than in non-tumor tissue [13, 14]. These data suggest that high circulating levels of leptin, and high levels of leptin produced locally in the tumor microenvironment may play a key role in the pathogenesis of BC.

In vitro studies demonstrated that leptin is a promoter of proliferation, migration and invasion, resistance to apoptosis and an inducer of epithelial-mesenchymal transition in several cancer-derived cell lines, including BC [15–18]. Epithelial-mesenchymal transition (EMT) is a process of transdifferentiation by which epithelial cells acquire a mesenchymal phenotype, characterized by a high migratory and invasive capacity, the progressive loss of epithelial markers such as E-cadherin, occludins, claudins, and gain of mesenchymal markers such as vimentin, N-cadherin, matrix metalloproteases, and transcription factors such as Snail, Slug, Twist and Zeb [19, 20].

It has been shown that acute leptin treatment induces EMT in several breast cancer-derived cell lines [17, 18, 21]. Moreover, acute leptin treatment induces partial EMT in MCF10A mammary epithelial cells through FAK and ERK signaling [22]. Leptin-induced partial EMT is characterized by a mesenchymal phenotype without the loss of cell–cell junctions, and at the molecular level by an increased expression of mesenchymal markers but without loss of E-cadherin [22, 23]. Chronic exposure of breast epithelial cells to high circulating levels of leptin and high leptin levels in the mammary gland in women with overweight or obesity could promote activation of cellular transformation processes such as EMT [12, 24–26]. Thus, in this study we aimed to investigate the effect of chronic leptin treatment on EMT in non-tumorigenic mammary epithelial cells.

## Material and Methods

### Materials

Human recombinant leptin (L4146), Cytosine arabinoside (Ara C, C1768), and anti-Mouse IgG (A9044) were obtained from Sigma-Aldrich (St Louis, MO, USA). Antibodies against E-cadherin (sc-8426 and sc-7870), vimentin (sc-6260), and FAK (sc-558) antibodies were obtained from Santa Cruz Biotechnology (Santa Cruz, CA, USA). Antibodies against pERK (9101S), ERK (9107S), pAKT

(4060S), and AKT (9272S) were obtained from Cell Signaling Technology (Danvers, MA, USA). Antibodies against GAPDH (AC027) and Bax (A0207) were obtained from ABclonal Technology (Woburn, MA, USA). Antibody against  $\alpha$ -tubulin (05–829) was obtained from Merck Millipore. Antibody against pFAK (44-624G), anti-Rabbit IgG (65–6120), anti-Mouse IgG Alexa Fluor 488 (A-11001) were obtained from Invitrogen. Rhodamine-Phalloidin (R415) was obtained from Thermo Scientific. Matrigel (356234) was obtained from Corning (Kennebunk, ME, USA).

### Cell Culture and Stimulation

The non-tumorigenic mammary epithelial cell line MCF10A (ATCC, Manassas, VA, USA) was cultured in DMEM/F12 medium (D8900, Sigma-Aldrich) supplemented with 5% fetal bovine serum (FBS) (By Productos, Guadalajara, Jal, Mexico), 10  $\mu$ g/mL insulin (Humulin R, Lilly), 0.5  $\mu$ g/mL hydrocortisone (H0888, Sigma-Aldrich), 20 ng/mL EGF (E5036, Sigma-Aldrich) and antibiotic–antimycotic (15240, Gibco) at 37 °C in a humidified atmosphere containing 5% CO<sub>2</sub>. The non-tumorigenic mouse mammary epithelial cell line EpH4-Ev (kindly provided by Paola Maycotte, CIBIOR-IMSS) was cultured in DMEM/F12 medium supplemented with 5% FBS at 37 °C in a humidified atmosphere containing 5% CO<sub>2</sub>. For chronic leptin treatment MCF10A and EpH4-Ev cells were cultivated with complete medium for 12 h. Then, the medium was replaced by complete medium plus 200 ng/mL or 400 ng/mL leptin, using 1% BSA (vehicle) as a control. Medium (containing vehicle or leptin) was changed every third day and cells were sub-cultured when reaching a confluence of 70–80%. Leptin treatment was continued for 28 days. Cell cultures were used between passages 2–15.

### Western Blot

Total protein extracts were obtained using Triton lysis buffer (50 mM Tris–HCl, 160 mM NaCl, 0.5 mM EDTA, 0.5 mM EGTA, 1% Triton X-100, 10% Glycerol) containing protease and phosphatase inhibitors (10 mM NaF, 1 mM PMSF, 1 mM Na<sub>3</sub>VO<sub>4</sub>). The total protein concentration was quantified using the Bradford protein assay (5000205, Bio-Rad). 30  $\mu$ g of total protein were separated by 10% SDS-PAGE and electrotransferred to a nitrocellulose membrane. After blocking in a TBS solution containing 3% BSA and 0.05% Tween-20 for 2 h, the membranes were incubated for 12 h at 4 °C with the primary antibodies: anti-GAPDH and anti- $\alpha$ -tubulin, 1:5000 dilution; all the other primary antibodies, 1:1000 dilution. The membranes were incubated with HRP-conjugated secondary antibody (anti-Mouse and anti-Rabbit

at 1:5000 dilution for 2 h at room temperature (RT), and protein bands were detected using a chemiluminescent kit (34577, Thermo Fisher Scientific) and autoradiography films (Carestream/Kodak). The relative protein level was determined by densitometric analysis of the bands using Image J software (NIH, Bethesda, MD, USA).

## Immunofluorescence and F-actin Staining

MCF10A cells were seeded on glass coverslips and grown to 70% confluence. Cells were fixed and permeabilized with a 4% formaldehyde/0.5% Triton X-100 solution for 15 min at 37 °C. For immunofluorescence (IF) assays, cells were blocked with 3% BSA in PBS 1X for 12 h at 4 °C. Then, the cells were incubated with the primary antibody at a 1:200 dilution for 2 h at RT, followed by incubation with anti-mouse Alexa 488 secondary antibody at 1:400 dilution for 2 h at RT. For F-actin staining, cells were incubated with Rhodamine-Phalloidin at 1:1000 dilution for 30 min at 37 °C. Nuclei were counterstained with DAPI using Fluoroshield™ mounting medium (F6057, Sigma-Aldrich). Images were captured with an Olympus BX43 microscope (Olympus Corporation; Allentown, PA, USA) using a 40× objective and analyzed with Image J software.

## Wound Healing Migration Assay

MCF10A cells were grown on 60-mm culture dishes until they reached 100% confluence. Cells were starved for 4 h in DMEM/F12 without FBS and treated for 2 h with 10 μM AraC, to inhibit proliferation. After treatment, the cell monolayer was scratch wounded using a sterile 200 μL pipette tip, washed twice to remove detached cells, re-fed with DMEM/F12 in the presence or absence of leptin. Cells were incubated for 48 h at 37 °C in a 5% CO<sub>2</sub> atmosphere. Following incubation, the cells were fixed with 4% formaldehyde. Phase-contrast images were acquired in an EVOs FL auto microscope (Life Technologies Corporation; Carlsbad, CA, USA) using a 10× objective and analyzed with Image J software.

## Matrigel Invasion Assay

Matrigel invasion assays were performed following the Transwell chamber method, in 24 well plates containing 8 μm pore size inserts (3464, Corning). Briefly, 100 μL of Matrigel were added to the top side of the inserts and kept at 37 °C for 1 h to form a semisolid matrix. MCF10A cells were treated for 2 h with 10 μM AraC, and 5 × 10<sup>5</sup> cells per insert were seeded on the top chamber in 200 μL serum-free

medium. The lower chamber was filled with 700 μL DMEM/F12 supplemented with 10% FBS. Cells were incubated for 48 h at 37 °C in a 5% CO<sub>2</sub> atmosphere. After 48 h, the cells and Matrigel on the upper surface of the Transwell membrane were gently removed with cotton swabs. Invading cells on the lower surface of the membrane were washed, fixed with 4% formaldehyde, and stained with 0.1% crystal violet diluted in PBS 1X. Images of the invading cells were acquired with an EVOs FL auto microscope using a 40× objective, and the number of invading cells was counted using Image J software.

## Hanging Drop Assay

For the hanging drop assay, MCF10A cells were trypsinized and resuspended in DMEM/F12 containing 10% FBS (plus insulin, hydrocortisone, EGF and antibiotic–antimycotic) at a density of 3500 cells/30 μL. Drops of 30 μL each, were placed on the inner part of a lid from a 60-mm culture dish. The lid containing the drops was inverted and placed on top of the dish containing sterile PBS 1X to maintain humidity and prevent evaporation of the hanging drops. Cells were maintained in non-adherent conditions (hanging-drops) for 48 h at 37 °C in a 5% CO<sub>2</sub> atmosphere. Then, phase-contrast photographs were acquired using an EVOs FL auto microscope with 20× objective. Cellular aggregation was analyzed by measuring the perimeter of the individual aggregates formed (size range 50–200 μm) within the drop using Image J software.

## Replating Efficiency

To determine the ability of cells recovered from the hanging drops to grow under adherent conditions, cells from 9 drops per condition were recovered, homogenized by repeated pipetting, and seeded in 60-mm culture dishes in complete medium with 10% FBS (plus insulin, hydrocortisone, EGF and antibiotic–antimycotic). Cell growth and morphology were monitored under an inverted microscope for 15 days. After 15 days of growing in adherent conditions, the number of viable cells was determined using trypan blue. The growth of leptin-treated cells was normalized to the number of control cells.

## Apoptosis Staining

To measure apoptosis on cells growing in non-adherent conditions (hanging drop) we used the Apoptosis Detection Kit (ab176749; Abcam) according to manufacturer's instructions. Briefly, MCF10A cells recovered from 9 hanging

drops were trypsinized and resuspended in a fixative solution (PBS 1X with 2% formaldehyde). The cells were washed with PBS 1X, centrifuged at  $500\times g$  for 5 min at 4 °C, resuspended in 50  $\mu\text{L}$  of Assay Buffer and 0.5  $\mu\text{L}$  of Apopxin Green Indicator (100X) and incubated at RT for 60 min in the dark. Cells were centrifuged at  $500\times g$  for 5 min at 4 °C, washed with 50  $\mu\text{L}$  Assay Buffer and counterstained with DAPI using Fluoroshield™ mounting medium. Images were captured with an Olympus BX43 microscope using a 40 $\times$  objective, and the quantification of green-fluorescent signal per cell was analyzed with Image J software. The procedure for the quantitative analysis of apoptotic cells is described in Fig S1.

## Bioinformatic Analysis

We selected two publicly available RNAseq datasets including samples from normal breast tissue obtained from women without breast cancer. The first dataset ‘‘Adipocyte and Active transcriptome in normal, healthy breast tissue from Komen Tissue Bank’’ generated by Kang et al. [27] (Available at Xena Platform [28]) contains RNAseq data from normal breast samples from 145 healthy, parous, non-obese women. A table with count for the genes of interest was obtained directly from Xena platform. The second dataset (GSE164694) includes RNAseq data from disease-free breast tissue from 187 women at either high- or average risk for breast cancer. The study was downloaded from GEO repository (GSE164641) in the form of files containing number of reads per gene. The files for 187 patient samples were integrated into a count table. For plotting, the numbers have been log<sub>2</sub>-transformed. Plots have been created using the pheatmap library. The data were analyzed with the clinical information available with GSE164641, using the edgeR package. Data analysis was done based on a list of 24 genes related to the leptin signaling pathway (*LEP*, *LEPR*, *JAK2*, *STAT3*, *STAT5A*, *SOCS-3*), epithelial EMT-related markers (*CDH1*, *EPCAM*, *CLDN3*, *CLDN4*, *OCLN*), and mesenchymal EMT-related genes (*VIM*, *CDH2*, *CTNNB1*, *TWIST1*, *SNAI1*, *SNAI2*, *ZEB1*, *ZEB2*, *MMP2*, *MMP9*, *FN1*, *TGFB1*, *TGFBRI*).

## Statistical Analysis

Data are presented as the mean  $\pm$  standard deviation (SD). Statistical comparisons between groups were assessed with Student’s *t*-test or one-way ANOVA, followed by the Dunnett’s or Newman-Keuls test. For all experiments,  $p < 0.05$  was considered statistically significant. All analyses were performed using GraphPad Prism 6.0.

## Results

### Chronic Leptin Treatment Induces Changes in Cell Morphology and the Expression of EMT Markers in MCF10A Cells

Several studies show that acute and chronic leptin treatment induces EMT in BC cell lines [17, 18, 25]. Moreover, in normal breast MCF10A epithelial cells, acute leptin treatment induces partial EMT [22, 23]. However, chronic leptin treatment in non-tumoral breast epithelium-derived cell lines has not been explored. To establish the optimal conditions for chronic leptin treatment, MCF10A cells were treated with 400 ng/mL for 14 or 28 days, in serum-free medium or with 2% or 5% FBS (Fig. S2). Cells growing in serum-free conditions exhibited a low proliferation rate and an increase in the number of apoptotic cells compared to cells growing in the presence of FBS. Moreover, no changes in EMT markers were observed in these cells after leptin treatment (Fig. S2a, c–e). Cells grown in medium supplemented with 2% or 5% FBS had a similar growth rate, but changes in EMT markers (increased vimentin and reduction of E-cadherin levels) in response to leptin treatment were observed only in cells growing in 5% FBS (Fig. S2b–e); therefore, all further experiments were performed in medium supplemented with 5% FBS. To evaluate the effect of chronic-leptin treatment on the human mammary epithelial cell line MCF10A, cells were cultivated in the presence of 200 ng/mL or 400 ng/mL leptin, for 14 or 28 days. To determine the effect of chronic leptin treatment on the morphology of MCF10A cells, phase-contrast microscopy images were acquired after 14 and 28 days of leptin treatment (Fig. 1a). The cell aspect ratio was calculated as the ratio of the longitudinal axis (longer side) to the transversal axis (shorter side) (Fig. 1b). Vehicle-treated cells exhibited an epithelial morphology with a mean aspect ratio of 2.4. In contrast, cells treated with 200 or 400 ng/mL leptin exhibited an enlarged mesenchymal morphology with a significant increase in the mean aspect ratio (2.8 and 3.1, respectively). Similar results were observed in cells treated for 14 days (Fig. 1c) or 28 days (Fig. 1d). Interestingly, the increase in the mean aspect ratio in leptin-treated cells correlated with a dose-dependent increase in the percentage of cells with aspect ratio 4–8 and a decrease in cells with aspect ratio 1–2 (Fig. 1e). Although cells treated with 200 ng/mL or 400 ng/mL leptin for 14 or 28 days exhibited a slight decrease in E-cadherin protein levels, a statistically significant decrease in E-cadherin protein levels was observed only in cells treated with 400 ng/mL for 28 days (Fig. 1f, g). In addition, leptin-treated MCF10A cells show a significant dose-dependent increase in the protein levels of vimentin at 14 or 28 days of treatment (Fig. 1f, g).

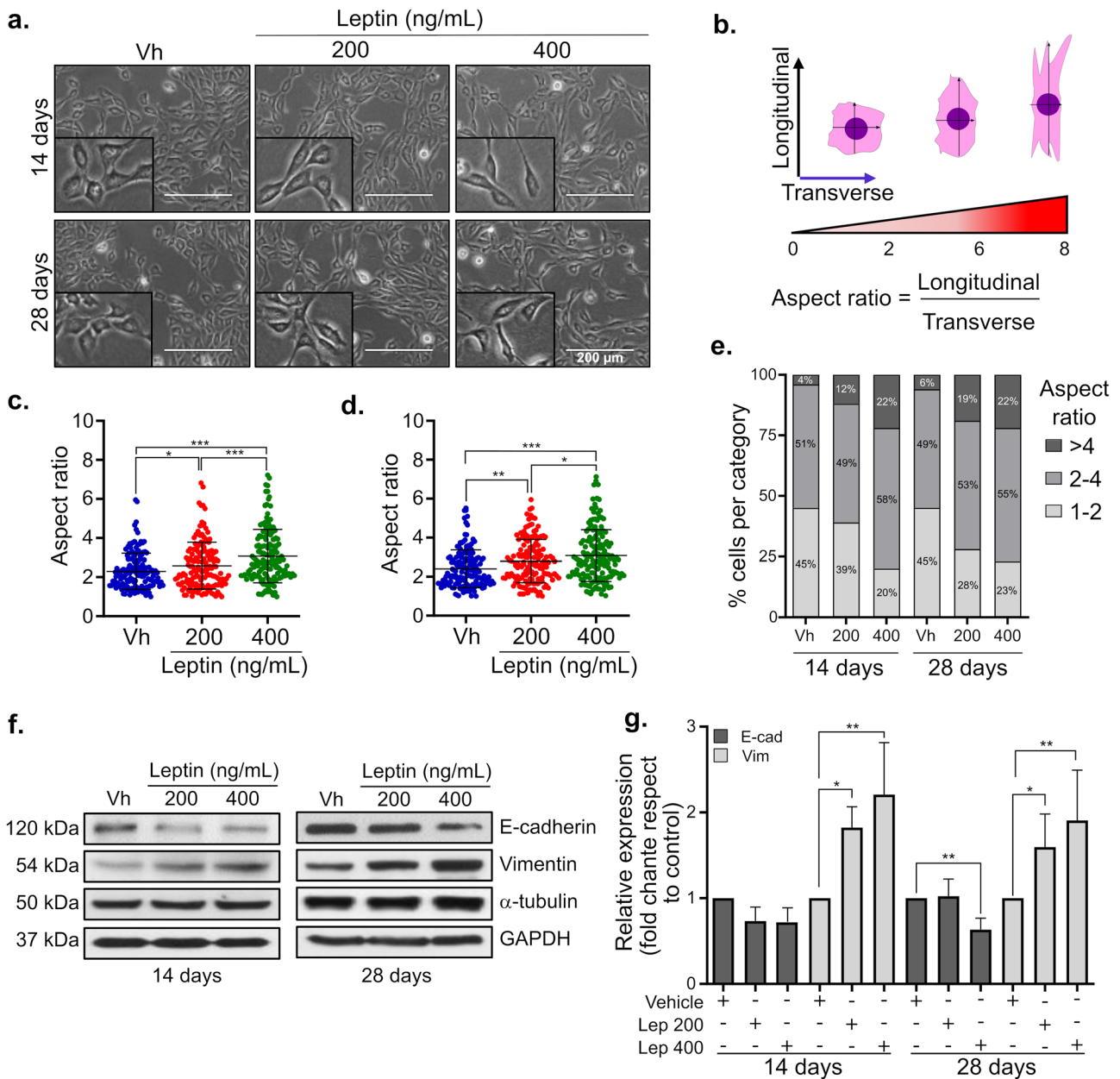


**Fig. 1** Chronic leptin treatment induces changes in cell morphology and in the expression of EMT markers in MCF10A cells. **(a)** Representative photographs of MCF10A cells treated with leptin for 14 or 28 days. Cells were cultured in complete medium with 200 ng/mL or 400 ng/mL leptin, or with vehicle (1% BSA as control) for 14 or 28 days. **(b)** Criteria used for determining the aspect ratio of each cell, defined as the ratio of the longitudinal axis to the transversal axis. **(c, d)** Distribution of individual cells according to their aspect ratio after 14 days **(c)** or 28 days **(d)** of leptin treatment. 150 cells

were counted in each group. Data are presented as the mean  $\pm$  SD. \* $p$ <0.05, \*\* $p$ <0.01, \*\*\* $p$ <0.001, one-way ANOVA (Newman-Keuls test). **(e)** Percentage of cells with aspect ratio 1–2, 2–4 or >4. **(f)** Relative levels of E-cadherin, vimentin,  $\alpha$ -tubulin, and GAPDH in MCF10A cells treated with 200 ng/mL or 400 ng/mL leptin, or with vehicle for 14 or 28 days. **(g)** The graphs show the fold change on protein levels, determined by the ratio to GAPDH and normalized to vehicle-treated cells. Data are presented as the mean  $\pm$  SD ( $n=3$ ). \* $p$ <0.05, \*\* $p$ <0.01, by one-way ANOVA (Dunnett’s test)

## Chronic Leptin Treatment Induces Loss of E-cadherin at Cell Junctions and Cytoplasmic Redistribution of Vimentin in MCF10A Cells

Loss of E-cadherin expression is a well-established event during EMT [29–31]. It has been reported that in MCF10A cells, acute leptin treatment induces changes in the subcellular localization of E-cadherin, with a reduction in its plasma membrane localization and an increase in the cytoplasmic pool of E-cadherin [22]. We analyzed the effect of chronic leptin treatment on E-cadherin subcellular localization in MCF10A cells. In vehicle-treated cells, a strong E-cadherin signal was observed at cell junctions, whereas in cells treated with leptin for 14 or 28 days there was a decrease in E-cadherin levels at the cell junctions (Fig. 2a). Quantification of E-cadherin signal showed a significant decrease of E-cadherin at cell junctions in cells treated with 200 ng/mL or 400 ng/mL leptin, compared to control cells (Fig. 2b), and a significant decrease in total E-cadherin signal intensity in cells treated with 400 ng/mL leptin, but not in cells treated with 200 ng/mL leptin (Fig. 2c). Overall, these results indicate that chronic leptin induces a decrease in E-cadherin protein levels and its localization at cell junctions in MCF10A cells.

Vimentin expression during EMT is associated with changes in cell shape, adhesion, and motility [32–34]. We analyzed the effect of chronic leptin treatment on the subcellular localization of vimentin in MCF10A cells. In vehicle-treated cells, approximately 50% of the cells exhibited vimentin filaments that were confined to the perinuclear area, and 50% of the cells show a dense, dispersed, and elongated distribution of vimentin filaments in the cytoplasm (Fig. 2d, e). A dose-dependent increase in the percentage of cells with cytoplasmic distribution of vimentin was observed in cells treated with 200 ng/mL or 400 ng/mL leptin (Fig. 2f). These results suggest that chronic leptin treatment promotes changes in the subcellular distribution in vimentin filaments in MCF10A epithelial cells.

## Chronic Leptin Treatment Increases Collective Cell Migration and Cell Invasion in MCF10A Cells

During EMT, epithelial cells may exhibit increased collective or individual migration capacity and acquire invasive properties [35–37]. We found that MCF10A cells treated with 200 ng/mL or 400 ng/mL leptin for 28 days, exhibited a significant increase in cell migration, compared to

vehicle-treated control cells, while maintaining their collective migration phenotype (Fig. 3a, b). Moreover, using Transwell Matrigel invasion assays, we found a significant dose-dependent increase in the invasion of MCF10A cells treated for 28 days with 200 ng/mL or 400 ng/mL leptin compared to vehicle-treated cells (Fig. 3c, d).

## Chronic Leptin Treatment Decreases Cell Aggregation of MCF10A Cells Growing in Suspension

EMT is characterized by decreased cell–cell adhesion and a loss of the cells ability to form aggregates [38, 39]. It has been shown that leptin treatment reduces cell aggregation of BC epithelial cells growing in suspension [25]. We performed hanging drop assays to assess the effect of chronic leptin treatment on the cell aggregation ability of MCF10A cells (Fig. 4a). Vehicle-treated cells formed spherical aggregates with well-defined edges and a compact distribution of the cells within the aggregate. In contrast, cells treated with leptin for 14 or 28 days, formed irregular aggregates showing a dispersed distribution of cells (Fig. 4b). Quantification of the cell aggregates perimeter showed a significant increase in the dispersion of the cells in the aggregates formed by leptin-treated cells compared to control cells (Fig. 4c). Interestingly, the decrease in cell aggregation was not observed in cells treated with leptin for 24 h (Fig. 4b, c).

## Chronic Leptin Treatment Induces Anoikis Resistance in MCF10A Cells

Previously, it has been reported that induction of EMT promotes resistance to anoikis, a type of apoptotic cell death induced by the loss of cell–cell and ECM–cell interactions [29, 40, 41]. To determine the effect of chronic leptin treatment on the viability of MCF10A cells growing in suspension, cells recovered from the hanging drops were stained with trypan blue. As shown in Fig. 5a, there was a significant increase in cell viability when the cells were treated with leptin for 14 or 28 days, but not when the cells were treated with leptin for 24 h. To determine if the increased viability in leptin-treated cells growing in suspension was due to a reduction in apoptosis, cell aggregates were collected and stained with the phosphatidylserine sensor Apopxin. We found that chronic leptin treatment induces a dose-dependent decrease in the number of Apopxin positive cells in the aggregates compared to vehicle-treated cells (Fig. 5b, c). In addition, chronic

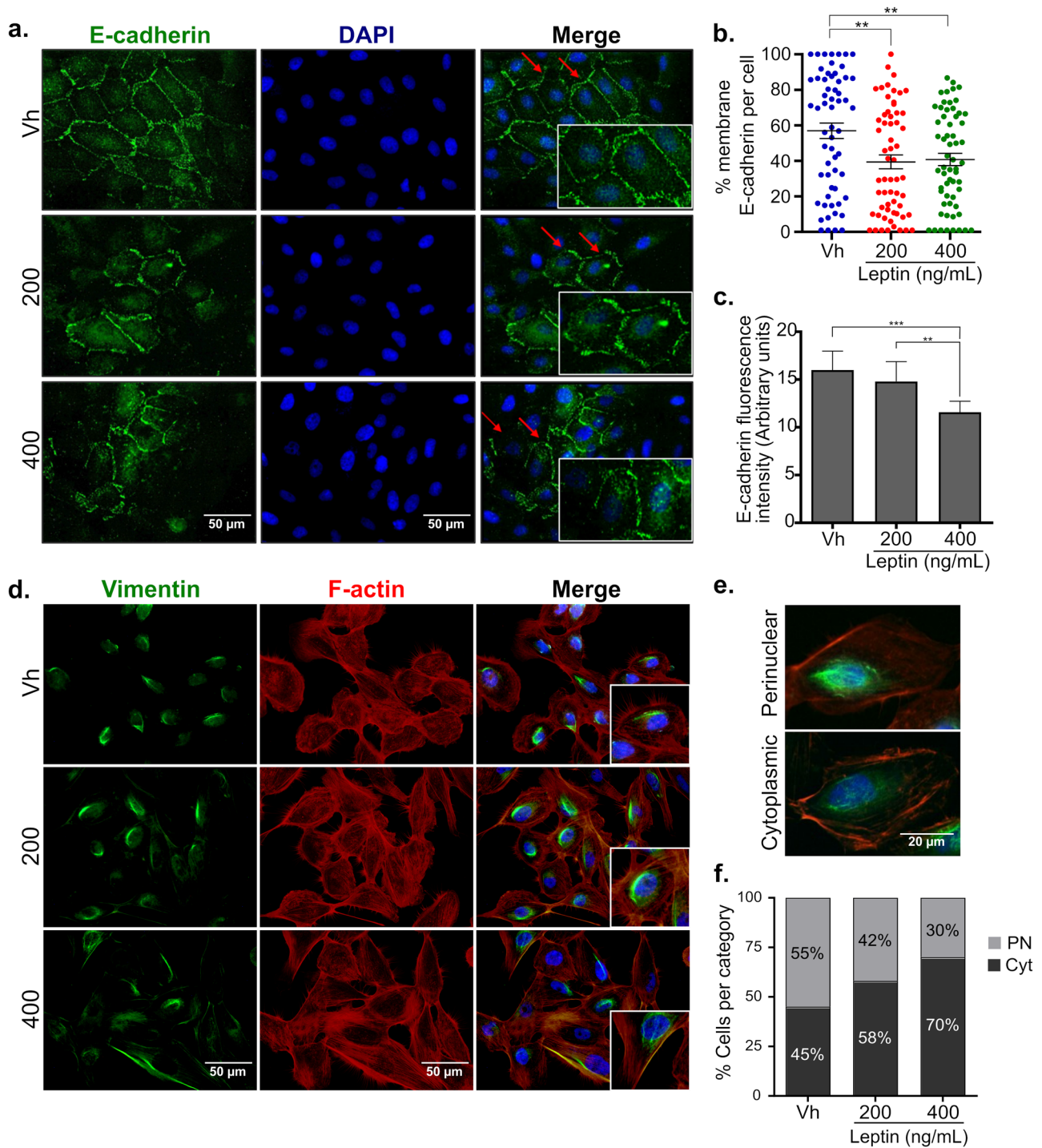


**Fig. 2** Chronic leptin treatment induced a decrease in E-cadherin at cell junctions and cytoplasmic redistribution of vimentin in MCF10A cells. **(a)** Representative fluorescence microscopy images of MCF10A cells treated with leptin or vehicle for 28 days showing E-cadherin (green) at cell junctions. Nuclei were stained with DAPI (blue). The images were captured with a 40 $\times$  objective. **(b)** Quantification and statistical analyses of the presence of E-cadherin at cell junctions. 60 cells per category were counted. **(c)** Quantification and statistical analyses of E-cadherin fluorescence intensity per cell. 10 cells per condition were counted. \*\* $p < 0.01$ , \*\*\* $p < 0.001$  by one-

way ANOVA (Newman-Keuls test). **(d)** Representative fluorescence microscopy images of MCF10A cells treated with leptin or vehicle for 28 days showing vimentin (green) and F-actin (red) distribution. Nuclei were stained with DAPI (blue). The images were captured using a 40 $\times$  objective. Insets in **(a)** and **(d)**: enlarged images showing representative areas of E-cadherin **(a)** or vimentin **(d)** subcellular localization. **(e)** Representative images showing the perinuclear and cytoplasmic distribution of vimentin filaments. **(f)** The graph shows the percentage of cells with perinuclear (PN) or cytoplasmic (Cyt) vimentin signal. 100 cells per condition were analyzed

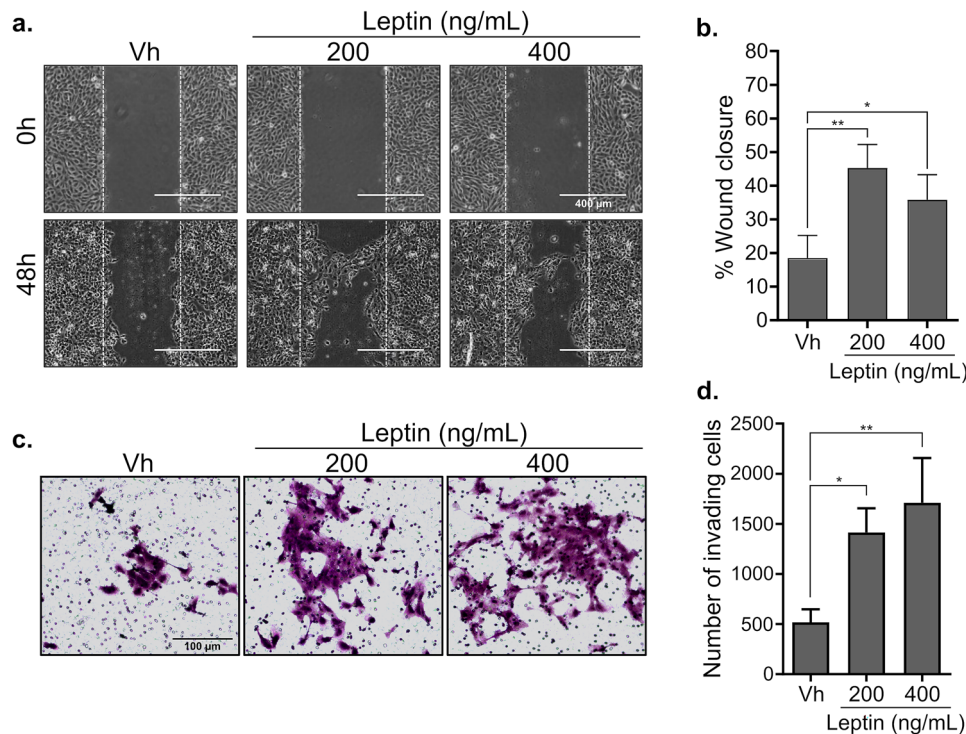


**Fig. 3** Chronic leptin treatment induces migration and invasion in MCF10A cells. **(a)** Representative phase-contrast microscopy images of wound healing experiments. MCF10A cells were treated with leptin or vehicle for 28 days until they reached 100% confluency, and a scratch wound was created on the cell monolayer. Images of the wound were acquired at 0 h and after 48 h with a 10 $\times$  objective. **(b)** The graph shows the percentage of wound closure for each experimental condition determined at 48 h. **(c)** Representative light micros-

copy images of invasion assays. MCF10A cells were treated with leptin or vehicle for 28 days, then seeded on Matrigel-coated Transwell inserts. After 48 h, the invaded cells were stained with crystal violet, and images acquired using a light microscope with a 40 $\times$  objective. **(d)** Quantitative analyses of the invasion assay showing the number of invading cells per category. Data in b and d are presented as the mean  $\pm$  SD ( $n = 3$ ). \* $p < 0.05$ , \*\* $p < 0.01$ , by one-way ANOVA (Dunnett's test)

leptin treatment also induced a significant reduction in the expression of the pro-apoptotic protein Bax in the cell aggregates (Fig. 5d).

### Leptin Treated Cells Recovered After Growing in Suspension Exhibit Increased Mesenchymal Phenotype

To determine the effect of chronic leptin treatment on the phenotype of the cells that survived in the hanging drop, cell aggregates were recovered and replated on adherent conditions (Fig. 6a). After 24 h growing on adherent conditions, vehicle-treated cells formed colonies with well-defined edges, with cells showing an epithelial morphology. In contrast, leptin-treated cells recovered from the hanging drops formed colonies with elongated cells at the edges. Similar results were obtained with cells treated with leptin for 24 h, 14 or 28 days (Fig. 6b). However, when the hanging drop-recovered cells were allowed to grow for 15 days under adherent conditions, leptin-treated cells

for 14 or 28 days exhibited a spindle-shaped phenotype and increased formation of stress fibers, compared to control cells (Fig. 6c). Moreover, a significant increase in the number of viable cells was observed in leptin-treated cells compared to control cells, after 15 days of growing under adherent conditions (Fig. 6d). This increase in the number of viable cells was not observed in cells treated with leptin for 24 h. To determine if the increased number of viable cells observed in leptin-treated cells after 15 days in adherent conditions was related to an increase in cell proliferation, cell aggregates recovered from the hanging drops were disaggregated and  $5 \times 10^5$  cells were seeded under adherent conditions, allowed to grow for 96 h, and cell viability was evaluated by trypan blue staining. No significant difference in the number of viable cells was observed between leptin-treated cells and control cells after 96 h growing in adherent conditions (Fig. 6e). Furthermore, leptin-treated cells recovered from the hanging drops exhibited a significant increase in the cell aspect ratio compared to vehicle-treated cells (Fig. 6f, g). As shown in Fig. 6h, leptin treatment induced a dose-dependent



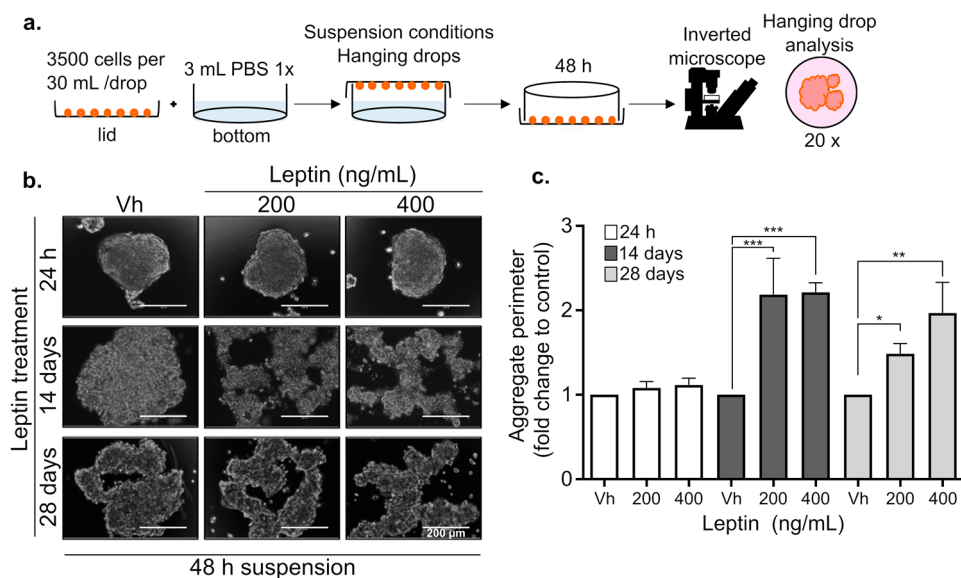


**Fig. 4** Chronic leptin treatment decreases cell aggregation of MCF10A. **(a)** Schematic representation of the hanging drop experiments. Nine drops containing 3500 cells in 30  $\mu$ L medium each were placed on the lid of a 60-mm culture dish. The lid was inverted on the culture dish containing 3 mL PBS 1X to maintain humidity and prevent evaporation of the hanging drops on the lid. The hanging drop culture was incubated for 48 h. **(b)** Representative microscopy images of cell aggregates from the hanging drop experiments. MCF10A cells

were treated with vehicle, with 200 ng/mL or 400 ng/mL leptin for 24 h, 14 days or 28 days, followed by 48 h in suspension condition. Cell aggregates were photographed using an inverted phase-contrast microscope with a 20 $\times$  objective. **(c)** The graph shows the average perimeter of the cellular aggregates in the hanging drop. Data are presented as the mean  $\pm$  SD (n = 3). \*\*p < 0.01, \*\*\*p < 0.001, by one-way ANOVA (Newman–Keuls test)

increase in the percentage of cells with mesenchymal morphology (Aspect ratio > 4), and a decrease in the percentage of cells with epithelial morphology (Aspect ratio 1–2).

### Chronic Leptin Treatment Increases FAK and AKT Activation in MCF10A Cells

It has been shown that the acquisition of mesenchymal characteristics such as increased migration, invasion and anoikis resistance is orchestrated through the action of various “master regulators” such as FAK, Src, PI3K/AKT, and ERK kinases [42–44]. To evaluate the effect of chronic leptin treatment in the activation of FAK, AKT and ERK in MCF10A cells, the phosphorylation levels of these kinases were determined by Western blot. As shown in Fig. 7, a significant increase in the levels of pFAK<sup>Y397</sup> was observed in cells treated with 200 ng/mL or 400 ng/mL of leptin for 24 h or 28 days (Fig. 7a, d). Moreover, increased levels of pAKT<sup>S473</sup> were observed in cells treated with 200 ng/mL or 400 ng/mL of leptin for 28 days, but not in cells treated for 24 h (Fig. 7b, e). In contrast, an increase in pERK1/2<sup>T202/Y204</sup> was observed in cells treated with 200 ng/mL of leptin for 24 h when compared to vehicle-treated cells, whereas a significant decrease was observed in cells treated for 28 days with 400 ng/mL of leptin (Fig. 7c, f).

### High Levels of Leptin Expression in Normal Breast Tissue Correlate with High Expression of Mesenchymal Genes and Low Expression of Epithelial Genes

Our results suggest that exposure of normal epithelial cells to high leptin levels may induce EMT in vivo. To explore if the leptin expression in normal breast tissue correlates with the expression of EMT-markers, we performed bioinformatic re-analysis of a publicly available dataset containing RNAseq data from normal breast biopsies from 145 healthy, parous, non-obese women [27]. We selected 6 genes from the leptin signaling pathway (LEP, LEPR, JAK2, STAT3, STAT5A, SOCS-3), 5 epithelial EMT-related markers (*CDH1*, *EPCAM*, *CLDN3*, *CLDN4*, *OCN*), and 11 mesenchymal EMT-related markers (*VIM*, *CDH2*, *CTNNA1*, *TWIST1*, *SNAI1*, *SNAI2*, *ZEB1*, *ZEB2*, *MMP2*, *MMP9*, *FN1*, *TGFB1*, *TGFBRI*) to perform subsetting of the full expression table for just the 24 selected genes. As shown in Fig. 8a, unsupervised clustering based on the 24 selected genes, revealed the presence of two main clusters, including a small cluster (cluster 1) containing samples with high levels of leptin and mesenchymal EMT-related genes, and low levels of epithelial EMT-related genes. Pearson’s correlation analysis shows the presence of three gene clusters, cluster 1

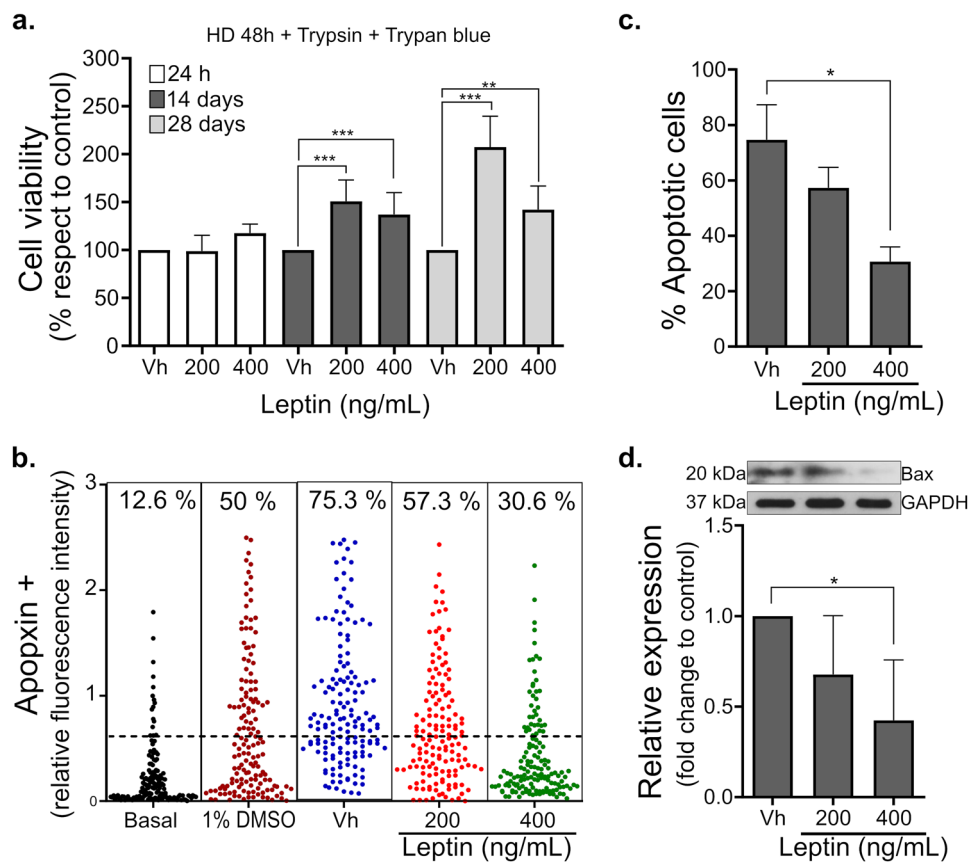


**Fig. 5** Chronic leptin treatment increases cell viability and reduces apoptosis under non-adherent conditions. **(a)** Cell viability in MCF10A growing in suspension. MCF10A cells were treated with leptin for 24 h, 14 days or 28 days and then grown in suspension for 48 h. The cell aggregates were trypsinized and stained with trypan blue. Data are presented as the mean  $\pm$  SD ( $n=3$ ).  $**p<0.01$ ,  $***p<0.001$ , by one-way ANOVA (Newman–Keuls test). **(b)** Quantification of apoptotic cells after 48 h in suspension conditions. After

48 h growing in suspension the cells were recovered from the drops, disaggregated, and stained with Apopxin. The number of Apopxin positive cells was determined by counting the cells under a fluorescence microscopy with a  $40\times$  objective. **(c)** The graph shows the percentage of apoptotic cells. **(d)** Bax protein levels in MCF10A cells growing in suspension. Cell aggregates were lysed with Triton lysis buffer and Bax protein levels were evaluated by WB. **(c, d)**  $*p<0.05$ , by one-way ANOVA (Dunnnett's test)

contains epithelial genes, cluster 2 includes genes from the leptin signaling pathway and mesenchymal genes. Interestingly, leptin is grouped with mesenchymal-related markers in cluster 3. Leptin showed a positive correlation with mesenchymal EMT-related markers, and a negative correlation with epithelial EMT-related genes (Fig. 8b). To further validate these observations, we performed a similar analysis on a second publicly available dataset (GSE164694), including RNAseq data from disease-free breast tissue from 187 women at either high- or average risk for breast cancer. As shown in Fig. 8c, unsupervised clustering of the samples based in the 24 selected genes identified a cluster including samples with high expression of leptin and mesenchymal EMT-related genes and low expression of epithelial EMT-related genes (cluster 1). Pearson's correlation showed a positive correlation between leptin and mesenchymal and leptin signaling genes (clusters 2 and 3) and a negative

correlation with epithelial genes (cluster 1) in this second dataset (Fig. 8d).

## Discussion

Leptin is a cytokine-like hormone that has been identified as a link between obesity and BC [6]. Obese people have high concentrations of circulating leptin and high leptin levels in the mammary gland, which can both promote the transformation of breast epithelial cells [11, 12, 24]. It has been shown that acute leptin treatment (24–96 h) induces EMT in BC cell lines and non-tumorigenic breast epithelial cell lines [17, 18, 21–23]. Leptin-induced EMT has also been demonstrated under chronic treatment conditions (14 days) in breast cancer cell lines (MCF7) and in Ha-Ras transformed MCF10A cells [25]. However, the

effect of chronic leptin treatment in the induction of EMT has not been evaluated in a non-tumorigenic background. Here, we assessed the effect of chronic leptin treatment on classical EMT markers and cellular characteristics in non-tumorigenic MCF10A cells.

EMT is characterized by a morphological transition from a polygonal/columnar phenotype (epithelial cells) to an elongated and spindle-shaped phenotype (mesenchymal cells). Here we found that chronic leptin treatment (14 and 28 days) induced a switch from epithelial to mesenchymal morphology. Vehicle-treated MCF10A cells could be classified into two major morphological groups, 45% of the cells exhibited a typical epithelial morphology (Aspect ratio 1–2), and ~50% of the cells showed a moderate mesenchymal morphology (Aspect ratio 2–4). Only a few cells showed a marked mesenchymal morphology (Aspect ratio > 4) (Fig. 1e). These observations are consistent with previous reports showing that MCF10A cells exhibit phenotypic heterogeneity, with some cells expressing epithelial markers (E-cadherin) and others expressing mesenchymal markers such as vimentin and N-cadherin [45–47]. Moreover, Gould et al. [47] demonstrated that under low serum conditions, TGF $\beta$  induces a mesenchymal phenotype, whereas stimulation with VEGF-A induces an epithelial phenotype in MCF10A. Interestingly, the co-stimulation with TGF $\beta$  and VEGF-A resulted in a heterogeneous population containing mesenchymal and epithelial cells [47]. Our experiments were performed in the presence of 5% FBS, which may contain TGF $\beta$  and VEGF-A, contributing to the phenotypic heterogeneity observed in the control cells. We found that chronic leptin treatment induced a dose-dependent reduction in the percentage of cells with epithelial morphology (Aspect ratio 1–2) and an increase in the number of cells with mesenchymal morphology (Aspect ratio > 4) (Fig. 1e). We observed similar results in Eph4-Ev cells, a non-tumorigenic cell line derived from spontaneously immortalized mouse mammary gland epithelial cells. In Eph4-Ev cells, leptin treatment induced an increase in the percentage of cells with mesenchymal morphology (Fig. S3a–c). Furthermore, a decrease in E-cadherin protein levels and a loss of E-cadherin at cell–cell contacts were observed in leptin-treated MCF10A cells (Fig. 1f, 2a). However, many cells still maintain E-cadherin expression at cell–cell junctions, which correlates with the observation that many cells show epithelial (20–40%) or intermediate (50–58%) morphology. Several studies have demonstrated similar changes in cell morphology and expression of E-cadherin in breast cancer cells lines in response to leptin [17, 18, 21].

Previous reports show that MCF10A cells treated with leptin for 24–72 h exhibited an elongated morphology and a membrane to cytoplasm relocation of E-cadherin, without reduction of the total levels of E-cadherin [22, 48]. Here, we found that leptin treatment for 14 or 28 days resulted

in a membrane to cytoplasm relocation of E-cadherin, and a decrease in the total E-cadherin levels (Fig. 2a, b). These data suggest that the relocation of E-cadherin to the cytoplasm precedes the reduction of E-cadherin protein levels, and that the decrease in E-cadherin protein levels is a late event during leptin-induced EMT in MCF10A cells. The progressive loss of E-cadherin in response to EMT inducers such as TGF $\beta$  and cadmium has been described in various cell types, including MCF10A cells [49–51]. The loss of E-cadherin can be regulated by its internalization and degradation mediated by interaction with proteins such as p120 and the E3 ubiquitin ligase Hakai [52], or through transcriptional repression at the promoter region by transcription factors such as  $\beta$ -catenin, Twist, Snail, and Zeb [53, 54]. Interestingly, acute leptin treatment induces a transient overexpression of  $\beta$ -catenin and Twist in MCF10A [23], which is not sufficient to induce a reduction of E-cadherin protein levels. Chronic leptin treatment may induce a sustained overexpression of these transcription factors in MCF10A cells, contributing to the observed decrease in E-cadherin levels during chronic leptin treatment.

Gain of vimentin expression is another hallmark of EMT. We found that chronic leptin treatment induced an increase of vimentin protein levels (Fig. 1f, g). Similar results were observed during acute leptin treatment [22]. In addition, leptin treatment induced a dose-dependent increase in the percentage of cells with cytoplasmic distribution of vimentin (Fig. 2f). These results correlated with the morphological observations showing that vehicle-treated cells are a mixture of epithelial/mesenchymal cells, and that leptin treatment increases the percentage of cells with mesenchymal morphology (Fig. 1e).

The increase in the migratory capacity of the cells during EMT occurs either as single cells, in a mesenchymal manner, or collectively retaining cell–cell contacts [20]. Our results show that chronic leptin treatment induces an increase in collective cell migration in MCF10A cells (Fig. 3a, b), which is characterized by the movement of cells interconnected by stable cell–cell junctions mediated mainly by cadherins [55]. Increased collective cell migration in response to chronic leptin was also observed in Eph4-Ev cells (Fig. S3d, e). Similar results were observed in MCF10A in which EMT was induced by Snail overexpression, where a combination of collective and individual migration could be observed [36]. Moreover, collective cell migration was also observed in MCF10A E-cadherin KO cells [56]. These data suggest that the loss of E-cadherin in non-tumorigenic breast cells during EMT, is not sufficient to induce a complete mesenchymal phenotype, and that a compensatory mechanism may be activated to maintain cell–cell adhesions during cell migration.

Interestingly, when MCF10A cells treated with leptin for 14 or 28 days were cultured in suspension (hanging drops)

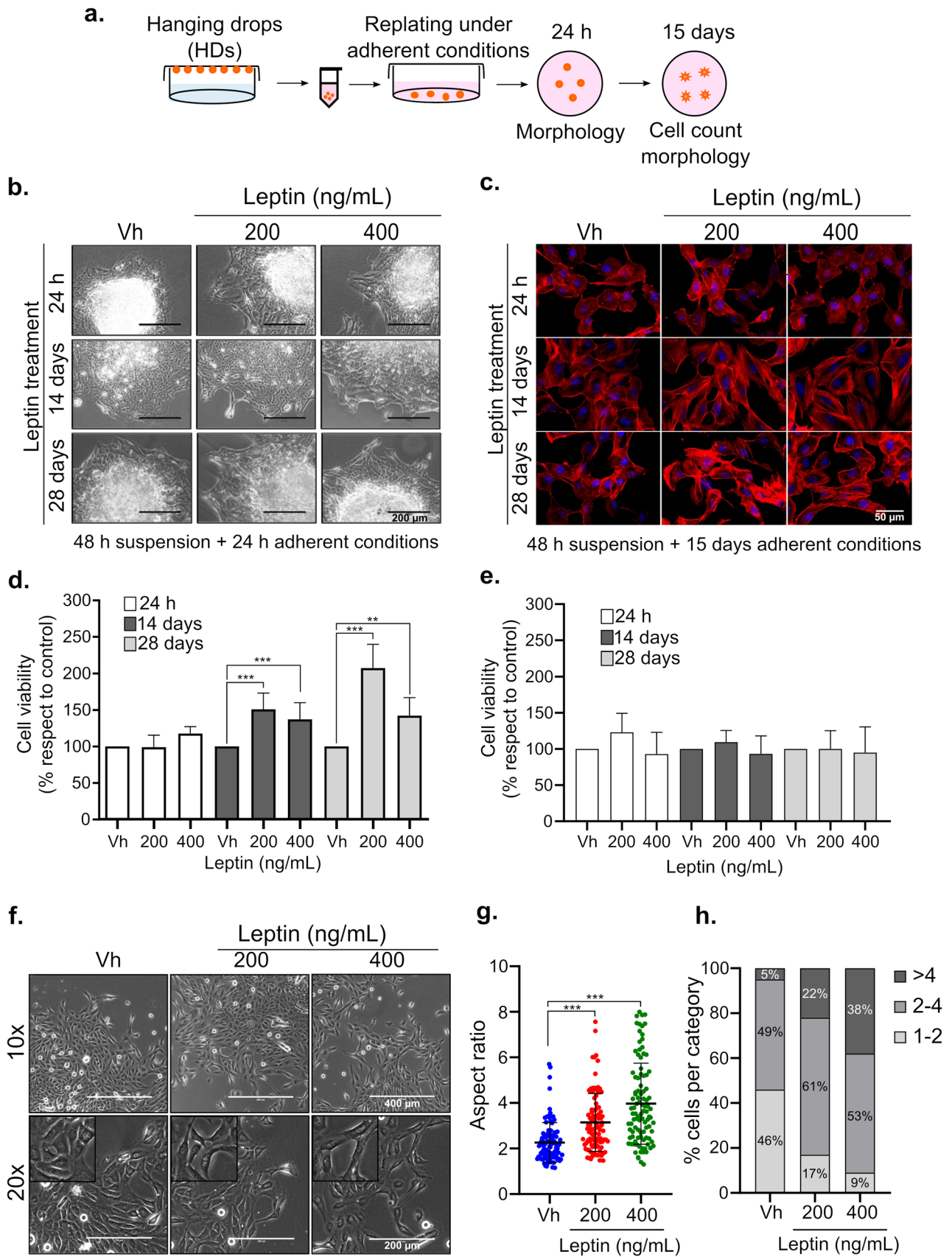


**Fig. 6** Leptin-treated cells recovered after growing in suspension exhibit an enhanced mesenchymal phenotype. **(a)** Schematic representation of the hanging drop recovery experiments. After 48 h growing in suspension conditions the cells from 9 hanging-drops (HDs) were recovered and plated under adherent conditions for 15 days. **(b)** Phase-contrast microscopy images from HDs-recovered cells after 24 h growing in adherent conditions. **(c)** Fluorescence microscopy images from HDs-recovered cells after 15 days growing in adherent conditions. Actin fibers were stained with Phalloidin (red) and nuclei stained with DAPI (blue). **(d)** Cell viability of HD-recovered cells after 15 days growing in adherent conditions. **(e)** After 48 h growing in suspension the cells from the HDs were disaggregated with trypsin, and  $5 \times 10^5$  cells per well were seeded on adherent conditions and grown for 96 h. Cell viability was determined by trypan blue. **(f)** Representative phase-contrast microscopy images of cells recovered from the HDs grown on adherent conditions for 12 days. **(g, h)** The graphs show the distribution of cell aspect ratio of HDs-recovered cells grown on adherent conditions for 12 days. Data are presented as the mean  $\pm$  SD ( $n=3$ ). \* $p < 0.05$ , \*\* $p < 0.01$ , \*\*\* $p < 0.001$ , by one-way ANOVA (Newman–Keuls test)

they exhibited a significant decrease in cell aggregation. Control cells formed compact spherical aggregates, whereas leptin-treated cells formed irregular aggregates (Fig. 4b, c). These effects were not observed in cells exposed to acute leptin treatment (24 h). In a recent report, Acheva et al. [48] demonstrated that leptin treatment for 14 days interferes with the formation of MCF10A 3D spheroids. They cultivated MCF10A cells in Matrigel for 14 days in the presence or not of leptin, and they found that, in contrast to control cells that formed well-organized spheroids, leptin-treated cells formed irregular structures [48]. Similarly, Mishra et al. [25] showed that chronic leptin treatment in MCF7 cells decreases cell aggregation in non-adherent conditions [25]. These data suggest that chronic exposure to leptin may affect the 3D organization of normal breast cells and breast cancer cells in vivo, contributing to the acquisition of migratory and invasive capacities.

It has been shown that leptin induces the activation of FAK, AKT and ERK pathways in non-tumorigenic breast epithelial cell lines and cancer cell lines [17, 22, 57]. The constitutive activation of FAK and AKT kinases has been associated with the acquisition of mesenchymal characteristics during TGF $\beta$ -induced EMT [58–60]. On the other hand, the activation of ERK kinase is essential for cell migration and anoikis resistance in MCF10A cells [22, 61, 62]. Here, we found that chronic leptin treatment induces the activation of FAK and AKT, but not of ERK in MCF10A cells (Fig. 7). Interestingly, we observed a significant decrease in ERK activation during chronic leptin treatment (Fig. 7c, f). These data suggest that induction of EMT by chronic leptin treatment in MCF10A cells is dependent on FAK and AKT activation but not on ERK activation.

Walker et al. [63] demonstrated that the constitutive activation of FAK in MCF10A cells resulted in enlarged

morphology, reduction of E-cadherin expression, increased migration, and suppression of apoptosis in 3D culture [63]. Here, we found that both acute and chronic leptin treatment increases FAK activation in MCF10A cells (Fig. 7a, d). However, leptin-induced survival in suspension was observed only in cells subjected to chronic leptin treatment (Fig. 5), suggesting that leptin-induced FAK activation is not sufficient to promote anoikis resistance in MCF10A cells. Interestingly, leptin treatment induced a dose-dependent increase in AKT phosphorylation in cells treated for 28 days but not in cells treated for 24 h (Fig. 7b, e). It has been shown that AKT can be activated either by integrin signaling which involves FAK and Src activation, or by an integrin-dependent pathway in response to growth factors [42, 64]. Moreover, it has been described that AKT activation by TGF $\beta$ 1 is independent of FAK signaling [65]. Because we found that FAK is activated during both chronic and acute leptin treatment, but AKT is activated only during chronic treatment, we suggest that AKT activation in response to leptin may occur by two independent pathways, being the FAK independent pathway the one involved in the acquisition anoikis resistance, which is only observed during chronic leptin treatment. In contrast, activation of both FAK and AKT pathways may be required for the EMT-related morphological changes induced by leptin and for the acquisition of migratory and invasive capacities. Further studies are required to elucidate the participation of FAK, AKT and ERK pathways in the leptin-induced acquisition of mesenchymal characteristics in MCF10A cells.

Recently, a gene expression signature in cancer-adjacent and histologically normal epithelium from breast cancer patients that correlates with poor overall survival in ER + breast cancer has been identified [66]. This active transcriptome phenotype is characterized by overexpression of genes related to cell movement, and downregulation of cell adhesion genes. Furthermore, samples with the active phenotype had more adipose tissue, suggesting that increase adiposity in the breast microenvironment could contribute to the active phenotype and increased risk of progression [67]. Recently, Kang et al. [27] demonstrated that this active transcriptome phenotype is present in normal breast tissue from healthy women without breast disease. Moreover, they found that samples with the active phenotype had increased adipose tissue as determined histologically (percentage of adipocyte nuclei and average adipocyte area). They also found that there is overexpression of leptin and leptin receptor in samples with active phenotype. Interestingly, when we performed unsupervised clustering of the RNA seq dataset from Kang et al. [27] based on a 24 gene signature, including EMT-related genes and leptin signaling genes, we found a cluster of samples with high expression of leptin and mesenchymal EMT-related gene, and low expression of epithelial EMT-related genes. Similar results were

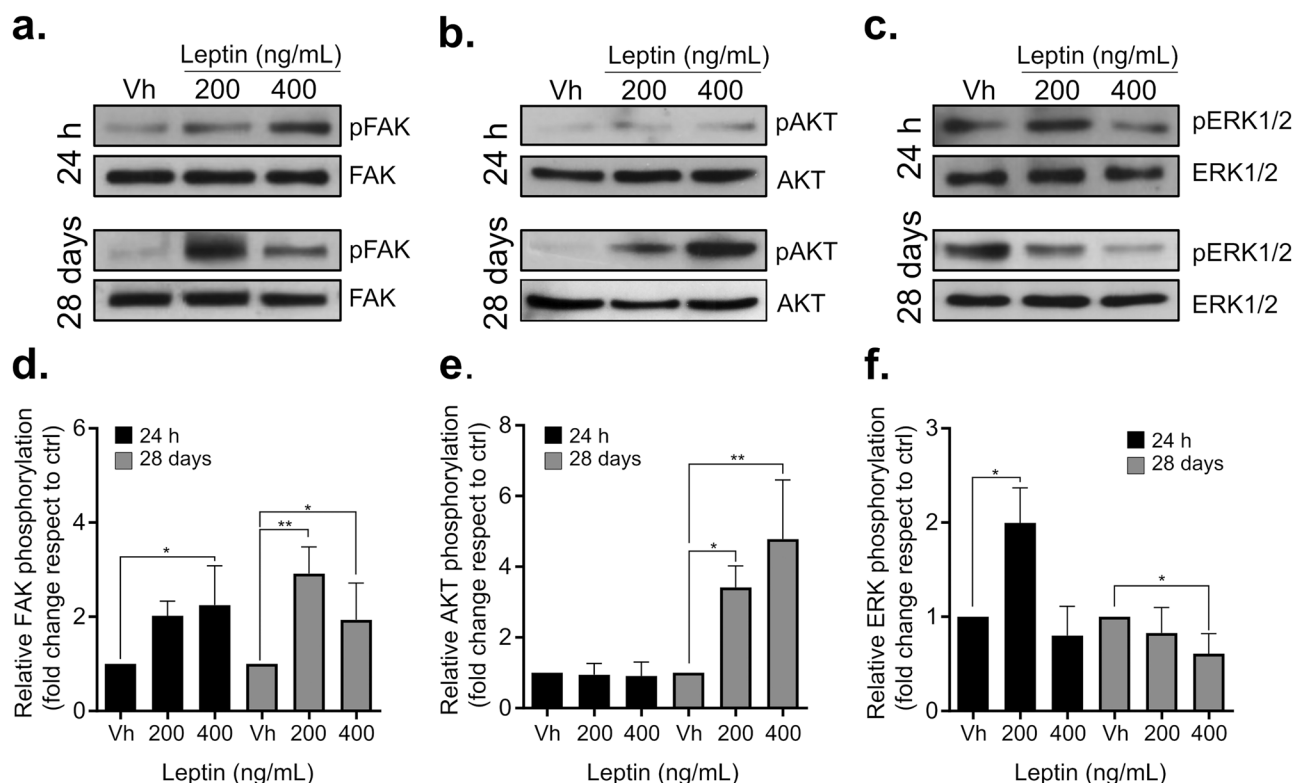


**Fig. 7** Chronic leptin treatment induces FAK and AKT phosphorylation in MCF10A cells. Relative phosphorylation of pFAK<sup>Y397</sup> (a), pAKT<sup>S473</sup> (b) and pERK1/2<sup>T202/pY204</sup> (c) determined by Western blot. MCF10A cells were treated with 200 ng/mL or 400 ng/mL leptin, or vehicle for 24 h or 28 days. Graphs show the fold change on the phos-

phorylation of pFAK<sup>Y397</sup> (d), pAKT<sup>S473</sup> (e) and pERK1/2<sup>T202/pY204</sup> (f) determined by the ratio to total FAK, AKT, or ERK1/2 levels, respectively and normalized to control cells (vehicle-treated cells). Data are presented as the mean  $\pm$  SD (n=3). \* $p < 0.05$ , \*\* $p < 0.01$ , \*\*\* $p < 0.001$ , by one-way ANOVA (Dunnett's test)

observed by analyzing a second publicly available dataset including 187 normal breast samples (Fig. 8a, c). Pearson's correlation shows a clear correlation between leptin expression and EMT-related genes in both datasets (Fig. 8b, d), including vimentin and E-cadherin (Fig. S4) which were found to be upregulated and downregulated after leptin treatment in MCF10A cells, respectively.

Recently, Delort et al. [68] demonstrated that co-culture of breast myoepithelial cells with preadipocytes or mature adipocytes results in a decrease in viability of breast myoepithelial cells (MECs) and suggest that this may play a role in cancer progression in vivo as MECs are considered to play a tumor suppressor role in BC. Interestingly, they found that MECs co-cultured with adipose cells had increased leptin expression. In line with these observations, using breast epithelial cells cocultured with adipose tissue explants derived from breast reduction mammoplasties, or exposed to leptin treatment, Tenvooren et al. [69] demonstrated that adipocytes or leptin treatment induced a loss in cell polarity of breast cells in 3D cultures. Here we show that chronic leptin treatment increases the proportion of cells with

mesenchymal morphology and the migratory properties of two non-tumorigenic breast cell lines (MCF10A and Eph4-Ev). Moreover, chronic leptin treatment increases vimentin expression and reduces E-cadherin expression in MCF10A cells, reduces cell aggregation and increases survival when the cells are grown in non-adherent conditions. Altogether, experimental data from non-tumorigenic breast epithelial cells and gene expression analysis in normal breast tissues strongly suggest that high levels of leptin production in the normal breast microenvironment by adipocytes, may induce the production of leptin by other non-fat cells such as myoepithelial or stromal cells [69, 70], further increasing the levels of leptin in the breast microenvironment. These high levels of leptin may contribute to establishing a pre-neoplastic microenvironment through several mechanisms including the establishment of an Active high-risk transcriptome phenotype, the disruption of MECs homeostasis and the induction of EMT in luminal epithelial cells. In the presence of carcinogenic events, this pre-neoplastic microenvironment may contribute to the development of breast tumors with increased invasive

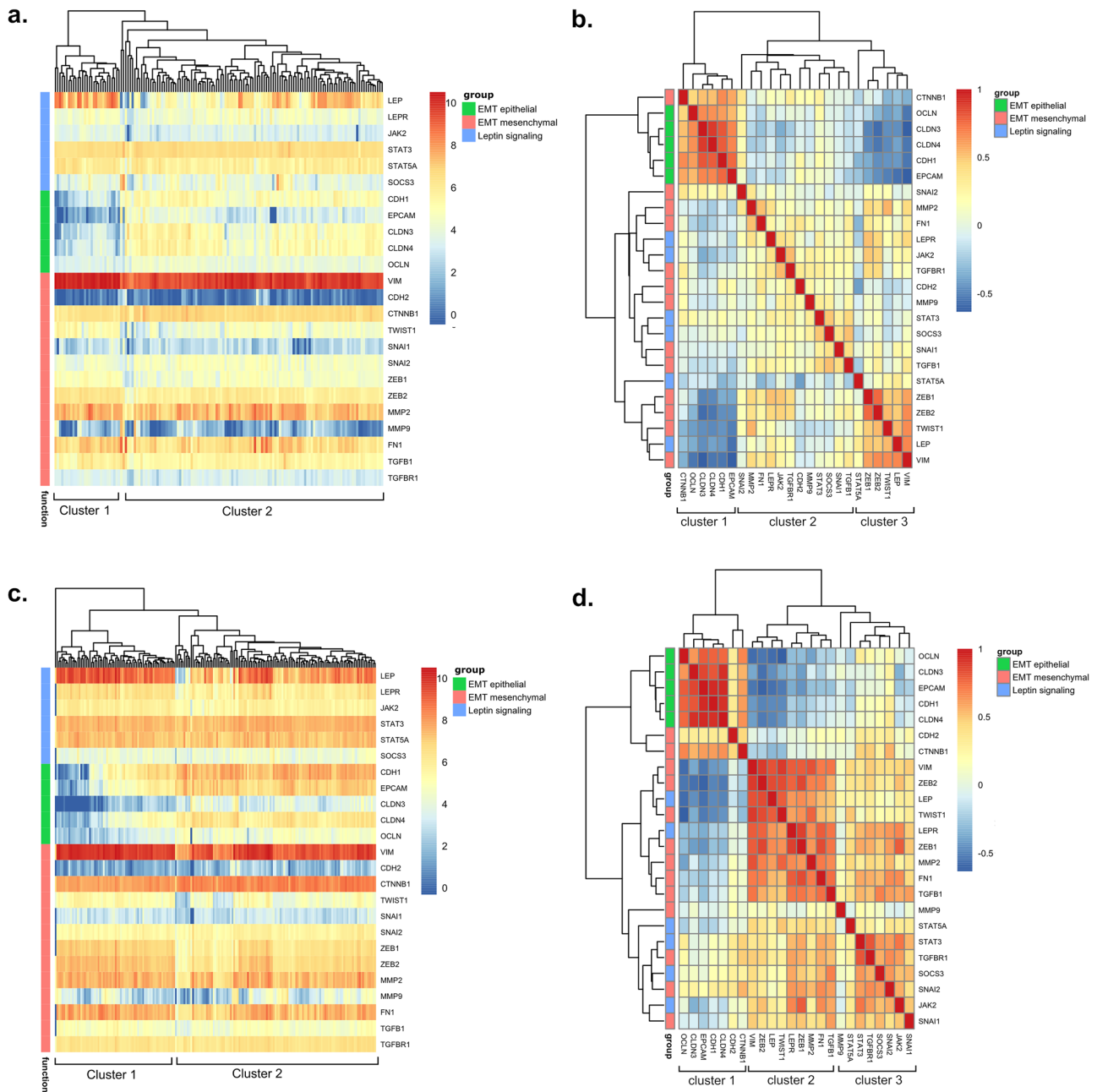


**Fig. 8** Leptin expression correlates positively with expression of mesenchymal EMT-related genes and negatively with epithelial genes in normal breast tissue. We explored two publicly available gene expression datasets containing RNA seq data from normal breast tissues (“Normal Breast” available at xena.uscs.edu) (**a, b**) and GSE164694. (**c, d**). Unsupervised clustering Heatmap of expression values (**a, c**) showing the presence of two main clusters. Cluster 1 is associated with high expression of leptin and mesenchymal-related genes, and

low expression of epithelial-related genes. (**b, d**) Heatmap of all the Pearson correlations were built based in the expression of 25 genes related to EMT and leptin signaling (**b, d**). heat map (red = increased gene expression, blue = decreased gene expression). In both datasets, genes are grouped into three clusters. Leptin shows a clear negative correlation with epithelial genes and positive correlation with mesenchymal and leptin-signaling genes

and metastatic potential. Finally, several lines of evidence demonstrate that leptin can also increase in the stem cell population in breast tumors and or cell lines [26, 68, 70, 71]. On the other hand, it has been shown that induction of EMT in normal breast epithelial cells results in the

acquisition of stem cell properties [72]. Whether leptin-induced EMT in non-tumorigenic normal breast cells can contribute to increasing stem cell population needs further investigation.

## Conclusions

In summary, this study shows that chronic leptin treatment induces EMT in MCF10A cells. Chronic leptin treatment increases the percentage of cells with mesenchymal morphology, induces collective cell migration and invasion, promotes survival, and reduces apoptosis of MCF10A cells growing in suspension. Moreover, in normal breast tissues, leptin expression correlates positively with mesenchymal markers and negatively with epithelial markers. Further studies are required to clarify the signaling pathways and biological implications of this chronic leptin-induced EMT in MCF10A cells and the biological relevance in vivo. Thus, our data suggest that the chronic exposure to elevated leptin levels present in normal breast tissue microenvironment may induce alterations in the normal mammary gland epithelium, that could predispose women to develop more aggressive breast tumors.

**Supplementary Information** The online version contains supplementary material available at <https://doi.org/10.1007/s10911-022-09515-9>.

**Authors' Contributions** JCJC, NNT and ECS contributed to the study conception and design. Material preparation, experimental procedures, and data collection were performed by JCJC. All authors contributed to data analysis and interpretation. JCJC, ECS contributed to RNAseq dataset selection and design of bioinformatic analyses, and MO performed RNAseq bioinformatic analysis and contributed to data interpretation. MR, COP contributed to data analysis and interpretation, and figure preparation. The first draft of the manuscript was written by JCJC and ECS, and all authors contributed to improving the final version of the manuscript. All authors read and approved the final manuscript.

**Funding** The project was founded by the “Programa de Fortalecimiento de la Calidad Educativa (PFCE)” awarded to Napoleón Navarro-Tito and Eduardo Castañeda-Saucedo (2018–2020). Juan Carlos Juárez-Cruz was awarded a PhD fellowship from the “Consejo Nacional de Ciencia y Tecnología (CONACYT)”, from 2018–2021.

**Availability of Data and Material** All data generated or analyzed in this work, and detailed experimental procedures are available upon request.

## Declarations

**Ethics Approval** Not applicable.

**Consent to Participation** Not applicable.

**Consent for Publication** Not applicable.

**Conflicts of Interest/Competing Interests** The authors have no conflicts of interest to declare that are relevant to the content of this article.

## References

- Nattenmüller CJ, Kriegsmann M, Sookthai D, Fortner RT, Steffen A, Walter B, et al. Obesity as risk factor for subtypes of breast cancer: Results from a prospective cohort study. *BMC Cancer*. 2018;18(1):1–8.
- Feigelson HS, Bodelon C, Powers JD, Curtis RE, Buist DSM, Veiga LHS, et al. Body Mass Index and Risk of Second Cancer among Women with Breast Cancer. *J Natl Cancer Inst*. 2021;113(9):1156–60.
- Blair CK, Wiggins CL, Nibbe AM, Storlie CB, Prossnitz ER, Royce M, et al. Obesity and survival among a cohort of breast cancer patients is partially mediated by tumor characteristics. *NPJ Breast Cancer*. 2019;5(1):1–7.
- Bhardwaj P, Brown KA. Obese Adipose Tissue as a Driver of Breast Cancer Growth and Development: Update and Emerging Evidence. *Front Oncol*. 2021;11:638918.
- Wu Q, Li B, Li Z, Li J, Sun S, Sun S. Cancer-associated adipocytes: Key players in breast cancer progression. *J Hematol Oncol*. 2019;12(1):1–5.
- Andò S, Gelsomino L, Panza S, Giordano C, Bonofiglio D, Barone I, et al. Obesity, leptin and breast cancer: Epidemiological evidence and proposed mechanisms. *Cancers*. 2019;11(1):62.
- Sánchez-Jiménez F, Pérez-Pérez A, de la Cruz-Merino L, Sánchez-Margalet V. Obesity and Breast Cancer: Role of Leptin. *Front Oncol*. 2019;9:596.
- Bahathiq S, Omar A. Relationship of leptin hormones with body mass index and waist circumference in Saudi female population of the Makkah Community. *Open Obes J*. 2010;2(1):95–100.
- Harris RBS. Direct and indirect effects of leptin on adipocyte metabolism. *Biochim Biophys Acta Mol Basis Dis*. 2014;1842(3):414–23.
- Niu J, Jiang L, Guo W, Shao L, Liu Y, Wang L. The Association between Leptin Level and Breast Cancer: A Meta-Analysis. *PLoS One*. 2013;8(6):e67349.
- Mohammadzadeh G, Ghaffari MA, Bafandeh A, Hosseini SM. Association of serum soluble leptin receptor and leptin levels with breast cancer. *Int J Res Med Sci*. 2014;19(5):433.
- Gu L, Di WC, Cao C, Cai LR, Li DH, Zheng YZ. Association of serum leptin with breast cancer. A meta-analysis *Medicine (Baltimore)*. 2019;98(5):e14094.
- Garofalo C, Koda M, Cascio S, Sulkowska M, Kanczuga-Koda L, Golaszewska J, et al. Increased expression of leptin and the leptin receptor as a marker of breast cancer progression: Possible role of obesity-related stimuli. *Clin Cancer Res*. 2006;12(5):1447–53.
- Karaduman M, Bilici A, Ozet A, Sengul A, Musabak U, Alomeroglu M. Tissue leptin levels in patients with breast cancer. *J BUON*. 2010;15(2):369–72.
- Xu M, le Cao F, Li N, Gao X, Su X, Jiang X. Leptin induces epithelial-to-mesenchymal transition via activation of the ERK signaling pathway in lung cancer cells. *Oncol Lett*. 2018;16(4):4782–8.
- Zhang B, Chen X, Xie C, Chen Z, Liu Y, Ru F, et al. Leptin promotes epithelial-mesenchymal transition in benign prostatic hyperplasia through downregulation of BAMBI. *Exp Cell Res*. 2020;387(1):111754.
- Yan D, Avtanski D, Saxena NK, Sharma D. Leptin-induced epithelial-mesenchymal transition in breast cancer cells requires  $\beta$ -catenin activation via AKT/GSK3- and MTA1/Wnt1 protein-dependent pathways. *J Biol Chem*. 2012;287(11):8598–612.
- Wang L, Tang C, Cao H, Li K, Pang X, Zhong L, et al. Activation of IL-8 via PI3K/AKT-dependent pathway is involved in leptin-mediated epithelial-mesenchymal transition in human breast cancer cells. *Cancer Biol Ther*. 2015;16(8):1220–30.
- Dongre A, Weinberg RA. New insights into the mechanisms of epithelial–mesenchymal transition and implications for cancer. *Nat Rev Mol*. 2019;20(2):69–84.
- Yang J, Antin P, Berx G, Blanpain C, Brabletz T, Bronner M, et al. Guidelines and definitions for research on epithelial–mesenchymal transition. *Nat Rev Mol*. 2020;21(6):341–52.



21. Wei L, Li K, Pang X, Guo B, Su M, Huang Y, et al. Leptin promotes epithelial-mesenchymal transition of breast cancer via the upregulation of pyruvate kinase M2. *J Exp Clin Cancer Res.* 2016;35(1):1–10.
22. Villanueva-Duque A, Zuniga-Eulogio MD, Dena-Beltran J, Castaneda-Saucedo E, Calixto-Galvez M, Mendoza-Catalán MA, et al. Leptin induces partial epithelial-mesenchymal transition in a FAK-ERK dependent pathway in MCF10A mammary non-tumorigenic cells. *Int J Clin Exp Pathol.* 2017;10(10):10334–42.
23. Olea-Flores M, Zuñiga-Eulogio M, Tacuba-Saavedra A, Bueno-Salgado M, Sánchez-Carvajal A, Vargas-Santiago Y, et al. Leptin Promotes Expression of EMT-Related Transcription Factors and Invasion in a SRC and FAK-Dependent Pathway in MCF10A Mammary Epithelial Cells. *Cells.* 2019;8(10):1133.
24. Hosney M, Sabet S, El-Shinawi M, Gaafar KM, Mohamed MM. Leptin is overexpressed in the tumor microenvironment of obese patients with estrogen receptor positive breast cancer. *Exp Ther Med.* 2017;13(5):2235–46.
25. Mishra AK, Parish CR, Wong M-L, Licinio J, Blackburn AC. Leptin signals via TGFβ1 to promote metastatic potential and stemness in breast cancer. *PLoS One.* 2017;12(5):e0178454.
26. Bowers LW, Rossi EL, McDonnell SB, Doerstling SS, Khatib SA, Lineberger CG, et al. Leptin signaling mediates obesity-associated CSC enrichment and EMT in preclinical TNBC models. *Mol Cancer Res.* 2018;16(5):869–79.
27. Kang T, Yau C, Wong CK, Sanborn JZ, Newton Y, Vaske C, et al. A risk-associated Active transcriptome phenotype expressed by histologically normal human breast tissue and linked to a pro-tumorigenic adipocyte population. *Breast Cancer Res.* 2020;22(1):1–15.
28. Goldman MJ, Craft B, Hastie M, Repčeka K, McDade F, Kamath A, Banerjee A, Luo Y, Rogers D, Brooks AN, Zhu J, Haussler D. Visualizing and interpreting cancer genomics data via the Xena platform. *Nat Biotechnol.* 2020;38(6):675–8. <https://doi.org/10.1038/s41587-020-0546-8>.
29. Onder TT, Gupta PB, Mani SA, Yang J, Lander ES, Weinberg RA. Loss of E-cadherin promotes metastasis via multiple downstream transcriptional pathways. *Cancer Res.* 2008;68(10):3645–54.
30. Moreno-Bueno G, Peinado H, Molina P, Olmeda D, Cubillo E, Santos V, et al. The morphological and molecular features of the epithelial-to-mesenchymal transition. *Nat Protoc.* 2009;4(11):1591–613.
31. Peixoto P, Etcheverry A, Aubry M, Missey A, Lachat C, Perrard J, et al. EMT is associated with an epigenetic signature of ECM remodeling genes. *Cell Death Dis.* 2019;10(3):1–17.
32. Mendez MG, Kojima S, Goldman RD. Vimentin induces changes in cell shape, motility, and adhesion during the epithelial to mesenchymal transition. *FASEB J.* 2010;24(6):1838–51.
33. Liu CY, Lin HH, Tang MJ, Wang YK. Vimentin contributes to epithelial-mesenchymal transition cancer cell mechanics by mediating cytoskeletal organization and focal adhesion maturation. *Oncotarget.* 2015;6(18):15966–83.
34. Leggett SE, Hruska AM, Guo M, Wong IY. The epithelial-mesenchymal transition and the cytoskeleton in bioengineered systems. *Cell Commun Signal.* 2021;19(1):1–24.
35. Pastushenko I, Blanpain C. EMT Transition States during Tumor Progression and Metastasis. *Trends Cell Biol.* 2019;29(3):212–26.
36. Wong IY, Javaid S, Wong EA, Perk S, Haber DA, Toner M, et al. Collective and individual migration following the epithelial-mesenchymal transition. *Nat Mater.* 2014;13(11):1063–71.
37. Aiello NM, Maddipati R, Norgard RJ, Balli D, Li J, Yuan S, et al. EMT Subtype Influences Epithelial Plasticity and Mode of Cell Migration. *Dev Cell.* 2018;45(6):681–95.e4.
38. Røslund GV, Dyrstad SE, Tusubira D, Helwa R, Tan TZ, Lotsberg ML, et al. Epithelial to mesenchymal transition (EMT) is associated with attenuation of succinate dehydrogenase (SDH) in breast cancer through reduced expression of SDHC. *Cancer Metab.* 2019;7(1):1–18.
39. Lourenço AR, Roukens MG, Seinstra D, Frederiks CL, Pals CE, Vervoort SJ, et al. C/EBPα is crucial determinant of epithelial maintenance by preventing epithelial-to-mesenchymal transition. *Nat. Commun.* 2020;11(1):1–18.
40. Huang RYJ, Wong MK, Tan TZ, Kuay KT, Ng AH, Chung VY, et al. An EMT spectrum defines an anoikis-resistant and spheroidogenic intermediate mesenchymal state that is sensitive to e-cadherin restoration by a src-kinase inhibitor, saracatinib (AZD0530). *Cell Death Dis.* 2013;4(11):e915.
41. Wang D, Zhang L, Hu A, Wang Y, Liu Y, Yang J, et al. Loss of 4.1N in epithelial ovarian cancer results in EMT and matrix-detached cell death resistance. *Protein Cell.* 2021;12(2):107–27.
42. Bouchard V, Demers MJ, Thibodeau S, Laquerre V, Fujita N, Tsuruo T, et al. Fak/SRC signaling in human intestinal epithelial cell survival and anoikis: Differentiation state-specific uncoupling with the PI3-K/AKT-1 and MEK/Erk pathways. *J Cell Physiol.* 2007;212(3):717–28.
43. Paoli P, Giannoni E, Chiarugi P. Anoikis molecular pathways and its role in cancer progression. *Biochim Biophys Acta Mol Cell Res.* 2013;1833(12):3481–98.
44. Yang J, Hou Y, Zhou M, Wen S, Zhou J, Xu L, et al. Twist induces epithelial-mesenchymal transition and cell motility in breast cancer via ITGB1-FAK/ILK signaling axis and its associated downstream network. *Int J Biochem Cell Biol.* 2016;71:62–71.
45. Sarrío D, Rodriguez-Pinilla SM, Hardisson D, Cano A, Moreno-Bueno G, Palacios J. Epithelial-mesenchymal transition in breast cancer relates to the basal-like phenotype. *Cancer Res.* 2008;68(4):989–97.
46. Qu Y, Han B, Yu Y, Yao W, Bose S, Karlan BY, et al. Evaluation of MCF10A as a reliable model for normal human mammary epithelial cells. *PLoS One.* 2015;10(7):e0131285.
47. Gould R, Bassen DM, Chakrabarti A, Varner JD, Butcher J. Population Heterogeneity in the Epithelial to Mesenchymal Transition Is Controlled by NFAT and Phosphorylated Sp1. *PLoS Comput Biol.* 2016;12(12):e1005251.
48. Acheva A, Kärki T, Schaible N, Krishnan R, Tojkander S. Adipokine Leptin Co-operates With Mechanosensitive Ca2+ Channels and Triggers Actomyosin-Mediated Motility of Breast Epithelial Cells. *Front Cell Dev Biol.* 2021;8:607038.
49. Dong C, Wu Y, Yao J, Wang Y, Yu Y, Rychahou PG, et al. G9a interacts with Snail and is critical for Snail-mediated E-cadherin repression in human breast cancer. *J Clin Investig.* 2012;122(4):1469–86.
50. Meyer-Schaller N, Cardner M, Diepenbruck M, Saxena M, Tiede S, Lüönd F, et al. A Hierarchical Regulatory Landscape during the Multiple Stages of EMT. *Dev Cell.* 2019;48(4):539–53.e6.
51. Chandrasekaran B, Dahiya NR, Tyagi A, Kolluru V, Saran U, Baby BV, et al. Chronic exposure to cadmium induces a malignant transformation of benign prostate epithelial cells. *Oncogenesis.* 2020;9(2):1–10.
52. Hartsock A, Nelson WJ. Competitive regulation of E-cadherin juxtamembrane domain degradation by p120-catenin binding and Hakai-mediated ubiquitination. *PLoS One.* 2012;7(5):e37476.
53. Fan X, Jin S, Li Y, Khadaroo PA, Dai Y, He L, et al. Genetic and epigenetic regulation of e-cadherin signaling in human hepatocellular carcinoma. *Cancer Manag Res.* 2019;11:8947–63.
54. Karimi Roshan M, Soltani A, Soleimani A, Rezaie Kahkhaie K, Afshari AR, Soukhtanloo M. Role of AKT and mTOR signaling pathways in the induction of epithelial-mesenchymal transition (EMT) process. *Biochimie.* 2019;165:229–34.
55. Friedl P, Gilmour D. Collective cell migration in morphogenesis, regeneration and cancer. *Nat Rev Mol Cell Biol.* 2009;10(7):445–57.
56. Chen A, Beetham H, Black MA, Priya R, Telford BJ, Guest J, et al. E-cadherin loss alters cytoskeletal organization and adhesion

- in non-malignant breast cells but is insufficient to induce an epithelial-mesenchymal transition. *BMC Cancer*. 2014;14(1):1–14.
57. Juárez-Cruz JC, Zuñiga-Eulogio MD, Olea-Flores M, Castañeda-Saucedo E, Mendoza-Catalán MÁ, Ortuño-Pineda C, et al. Leptin induces cell migration and invasion in a FAK-SRC-dependent manner in breast cancer cells. *Endocr Connect*. 2019;8(11):1539–52.
  58. Wendt MK, Schiemann WP. Therapeutic targeting of the focal adhesion complex prevents oncogenic TGF $\beta$  signaling and metastasis. *Breast Cancer Res*. 2009;11(5):1–16.
  59. Bae GY, Hong SK, Park JR, Kwon OS, Kim KT, Koo JH, et al. Chronic TGF $\beta$  stimulation promotes the metastatic potential of lung cancer cells by Snail protein stabilization through integrin  $\beta$ 3-AKT-GSK3 $\beta$  signaling. *Oncotarget*. 2016;7(18):25366–76.
  60. Katsuno Y, Meyer DS, Zhang Z, Shokat KM, Akhurst RJ, Miyazono K, et al. Chronic TGF $\beta$  exposure drives stabilized EMT, tumor stemness, and cancer drug resistance with vulnerability to bitopic mTOR inhibition. *Sci Signal*. 2019;12(570):eaau8544.
  61. Reginato MJ, Mills KR, Paulus JK, Lynch DK, Sgroi DC, Debnath J, et al. Integrins and EGFR coordinately regulate the pro-apoptotic protein Bim to prevent anoikis. *Nat Cell Biol*. 2003;5(8):733–40.
  62. Collins NL, Reginato MJ, Paulus JK, Sgroi DC, LaBaer J, Brugge JS. G 1 /S Cell Cycle Arrest Provides Anoikis Resistance through Erk-Mediated Bim Suppression. *Cell Mol Biol*. 2005;25(12):5282–91.
  63. Walker S, Foster F, Wood A, Owens T, Brennan K, Streuli CH, et al. Oncogenic activation of FAK drives apoptosis suppression in a 3D-culture model of breast cancer initiation. *Oncotarget*. 2016;7(43):70336–52.
  64. Beauséjour M, Noël D, Thibodeau S, Bouchard V, Harnois C, Beaulieu JF, et al. Integrin/Fak/SRC-mediated regulation of cell survival and anoikis in human intestinal epithelial crypt cells: Selective engagement and roles of PI3-K isoform complexes. *Apoptosis*. 2012;17(6):566–78.
  65. Horowitz JC, Rogers DS, Sharma V, Vittal R, White ES, Cui Z, et al. Combinatorial activation of FAK and AKT by transforming growth factor- $\beta$ 1 confers an anoikis-resistant phenotype to myofibroblasts. *Cell Signal*. 2007;19(4):761–71.
  66. Román-Pérez E, Casbas-Hernández P, Pirone JR, Rein J, Carey LA, Lubet RA, et al. Gene expression in extratumoral microenvironment predicts clinical outcome in breast cancer patients. *Breast Cancer Res*. 2012;14(2):1–12.
  67. Troester MA, Lee MH, Carter M, Fan C, Cowan DW, Perez ER, et al. Activation of host wound responses in breast cancer microenvironment. *Clin Cancer Res*. 2009;15(22):7020–8.
  68. Delort L, Cholet J, Decombat C, Vermerie M, Dumontet C, Castelli FA, et al. The Adipose Microenvironment Dysregulates the Mammary Myoepithelial Cells and Could Participate to the Progression of Breast Cancer. *Front Cell Dev Biol*. 2020;8:571948.
  69. Tenvooren I, Jenks MZ, Rashid H, Cook KL, Muhlemann JK, Sistrunk C, et al. Elevated leptin disrupts epithelial polarity and promotes premalignant alterations in the mammary gland. *Oncogene*. 2019;38(20):3855–70.
  70. Giordano C, Chemi F, Panza S, Barone I, Bonofiglio D, Lanzino M, et al. Leptin as a mediator of tumor-stromal interactions promotes breast cancer stem cell activity. *Oncotarget*. 2016;7(2):1262–75.
  71. Esper RM, Dame M, McClintock S, Holt PR, Dannenberg AJ, Swicha M, et al. Leptin and adiponectin modulate the self-renewal of normal human breast epithelial stem cells. *Cancer Prev Res (Phila)*. 2015;8(12):1174–83.
  72. Mani SA, Guo W, Liao MJ, Eaton EN, Ayyanan A, Zhou AY, et al. The Epithelial-Mesenchymal Transition Generates Cells with Properties of Stem Cells. *Cell*. 2008;133(4):704–15.

**Publisher's Note** Springer Nature remains neutral with regard to jurisdictional claims in published maps and institutional affiliations.